Electronic Supplementary Material (ESI) for Energy & Environmental Science.

Supplementary Information

High-performance silicon-based multicomponent battery anodes produced via synergistic coupling of multifunctional coating layers

Jung-In Lee, Younghoon Ko, Myoungsoo Shin, Hyun-Kon Song, Nam-Soon Choi,
Min Gyu Kim* and Soojin Park*

J.-I. Lee, Y. Ko, M. Shin, H.-K. Song, N.-S. Choi, S. Park
Department of Energy Engineering, School of Energy and Chemical Engineering, Ulsan National Institute of Science and Technology (UNIST), Ulsan 689-798, South Korea

M. G. Kim
Beamline Research Division, Pohang Accelerator Laboratory, Pohang University of Science and Technology, Pohang 790-784, South Korea

*Corresponding Authors:
Soojin Park, spark@unist.ac.kr
Min Gyu Kim, mgkim@postech.ac.kr

Table S1. Electrochemical properties of Si-based anode materials

Structure	**Synthetic methods**	**First charge capacity (mAh/g)**	**Capacity retention (%)**	**C-rate**	**Loading mass of active material (mg/cm^2)**	**Ref.**
Si nanoparticle	Commercial	~2500	65 (400 cycles)	0.5 C	0.2-0.3	*Adv. Mater.*, 2013, **25**, 1571.
Porous Si	Mg reduction	~1650	62.6 (1000 cycles)	0.5 C	0.5-1.0	*Sci. Rep.*, 2014, **4**, 5623.
Si-C yolk-shell	Carbon coating on Si-SiO_2 core-shell and etching	1180	98.3 (1000 cycles)	0.5 C	0.2	*Nat. Nanotechnol.*, 2014, **9**, 187.
	Air inflation	1650	65 (40 cycles)	0.5 C	N/A	*RSC Adv.*, 2014, **4**, 36218.
Si nanowire	Template-based impregnation	~3000	33.5 (1000 cycles)	0.5 C	0.03-0.04	*Nano Lett.*, 2013, **13**, 5740.
Si nanotube	Mg reduction of SiO_2 nanotubes	~1850	48.6 (90 cycles)	0.1 C	N/A	*Adv. Mater.*, 2012, **24**, 5452.
Ti_xSi_y-coated Si/Al_2O_3 nanotube	Coaxial-electrospinning and Al reduction	1540	75 (280 cycles)	0.5 C	1.59	Nanoscale, 2015, 7, 6126.
Si/C	CVD	1950	>95 (100 cycles)	1.0 C	N/A	Nat. Mater. 2010, 9, 353.
Si NP-PANi composite	In-situ polymerization	2500	55 (1000 cycles)	1.0 C	0.2-0.3	Nat. Commun. 2013, 4, 1943.
Si pomegranate	Microemulsion	2350	>99 (1000 cycles)	0.5 C	0.2	Nat. Nanotechnol. 2014, 9, 187.
3D porous Si/C	Template-based chemical reduction	2820	90 (100 cycles)	1.0 C	N/A	Angew. Chem. Int. Ed. 2008, 47, 10151.
3D porous Si/SiOx/C	Chemical etching/thermal decomposition	1600	>99 (100 cycles)	0.2 C	1.2	Angew. Chem. Int. Ed. 2012, 51, 2767.
Si-based multicomponent	Sol-gel process	900	>65 (1000 cycles)	1.0 C	1.5	This study

Figure S1. (a) HAADF-STEM image of the Si-multi-50 particles with lithium silicate and lithium titanate coating layers. Elemental mapping analysis of (b) Si, (c) O, and (d) Ti elements. (e) Elemental line mapping of the Si-multi-50 from the outer shell to core until the depth of around 100 nm. (f) Intensity of each element obtained as a function of distance. From the depth of ~45 nm, intensity of Ti element was abruptly decreased, while Si and O slightly increased. This result indicates that new layers, lithium silicate, are spatially located at the interface between Si core and lithium titanate shell.

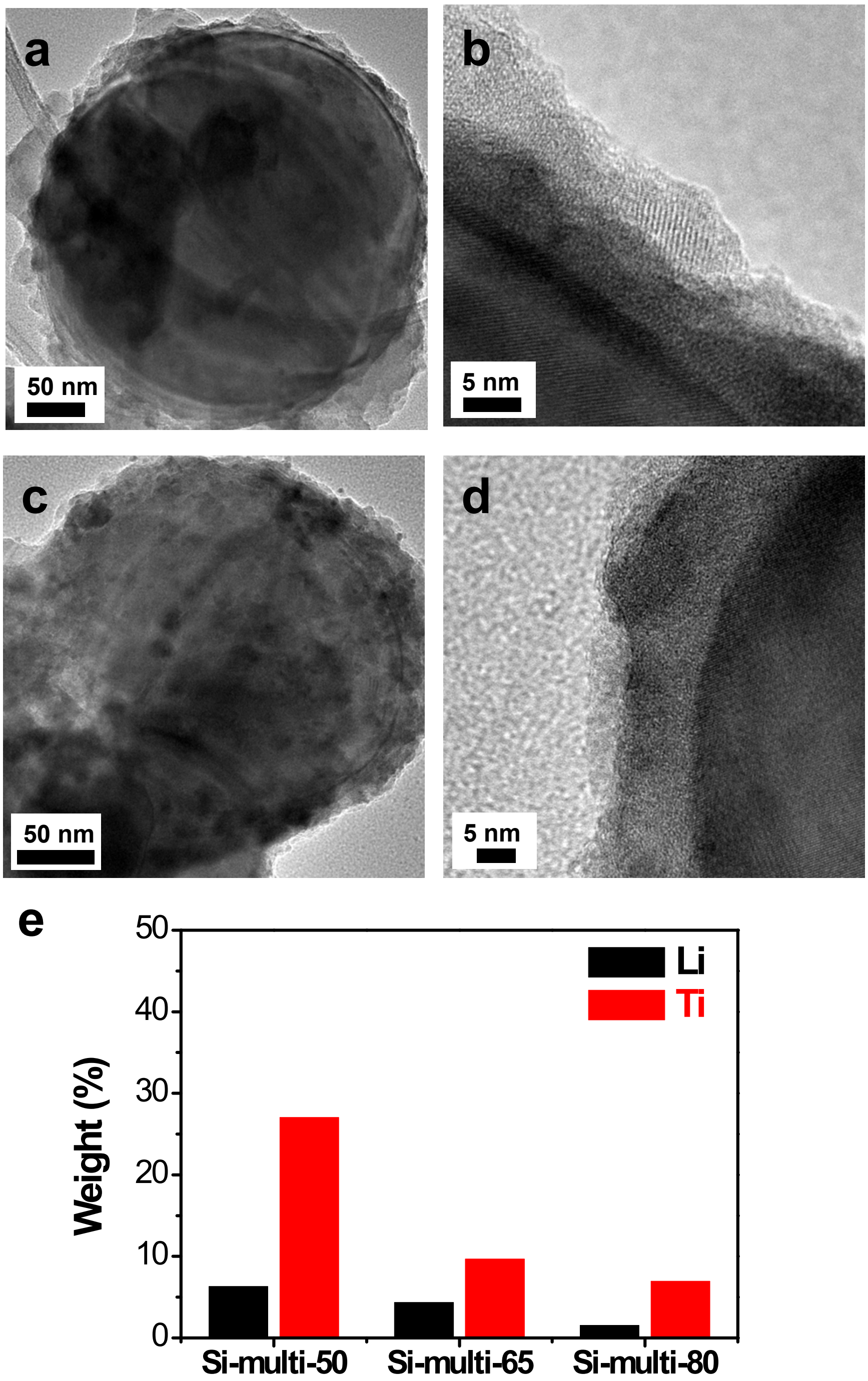

Figure S2. (a) TEM image of Si-multi-65 synthesized with molar ratio of Ti:Li:Si = 2.5:4:17 and (b) its magnification showing Si covered with 15 nm thick multifunctional coating layers. (c) TEM image of Si-multi-80 (molar ratio: Ti:Li:Si = 1.25:2:17) and (d) its magnification showing Si covered with 12 nm thick coating layers. (e) The contents of Li and Ti in Si-multi-50, Si-multi-65, and Si-multi-80 samples obtained through inductively coupled plasma atomic emission spectroscopy (ICP) analysis

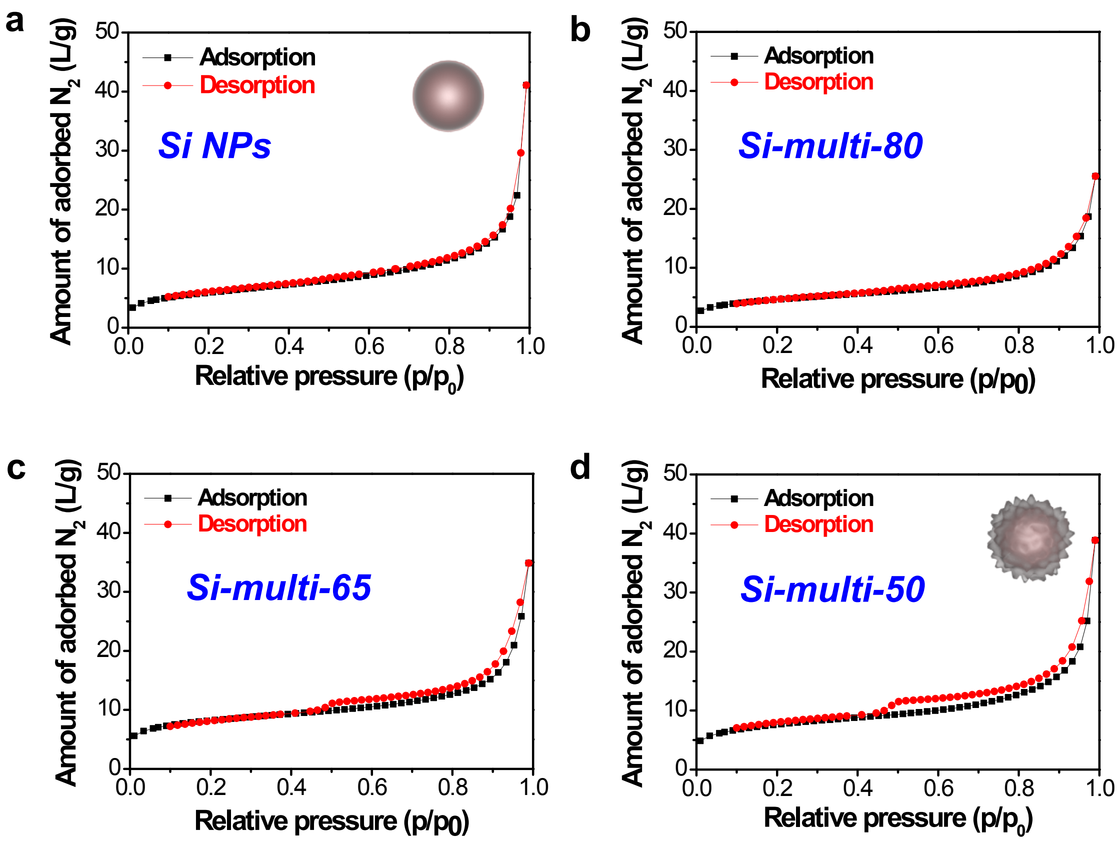

Figure S3. Specific BET surface areas of pristine Si and Si-multicomponents. (a) Nitrogen adsorption-desorption curves of (a) pristine Si, (b) Si-mul-80, (c) Si-multi-65, and (d) Si-mul-50. The Si-multicomponents show a typical adsorption-desorption hysteresis curve indicating macro/mesoporous structure, while the pristine Si exhibits non-porous structure.

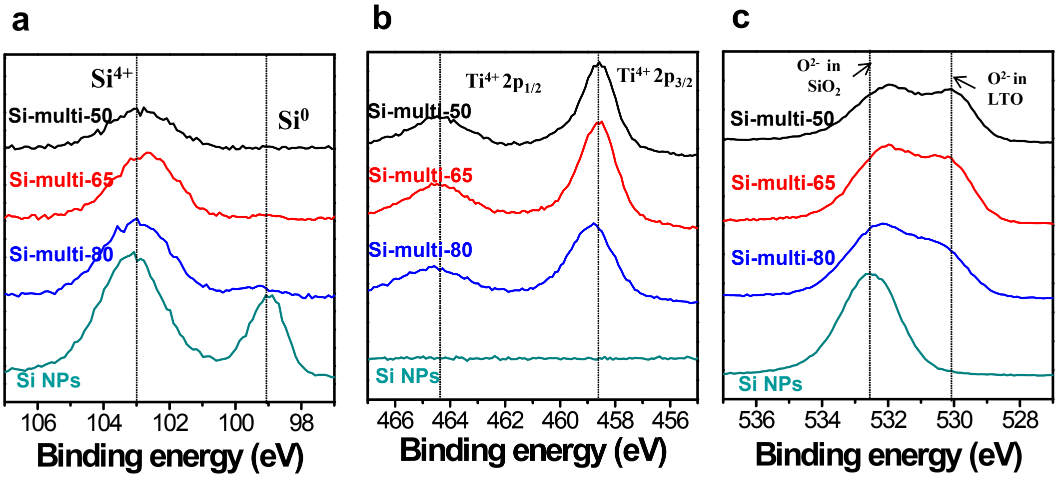

Figure S4. XPS characterization of pristine Si, Si-multi-50, Si-multi-65, and Si-multi-80 particles. XPS spectra of (a) Si 2p, (b) Ti 2p and (c) O 1s of the Si-based materials. The Si-multicomponents have only one peak at around 103 eV for Si^{4+} due to multi-coating layer on Si surface. Additionally, we confirmed that lithium titanium and lithium silicate exist on the Si surface as shown in Fig. S4b and S4c.

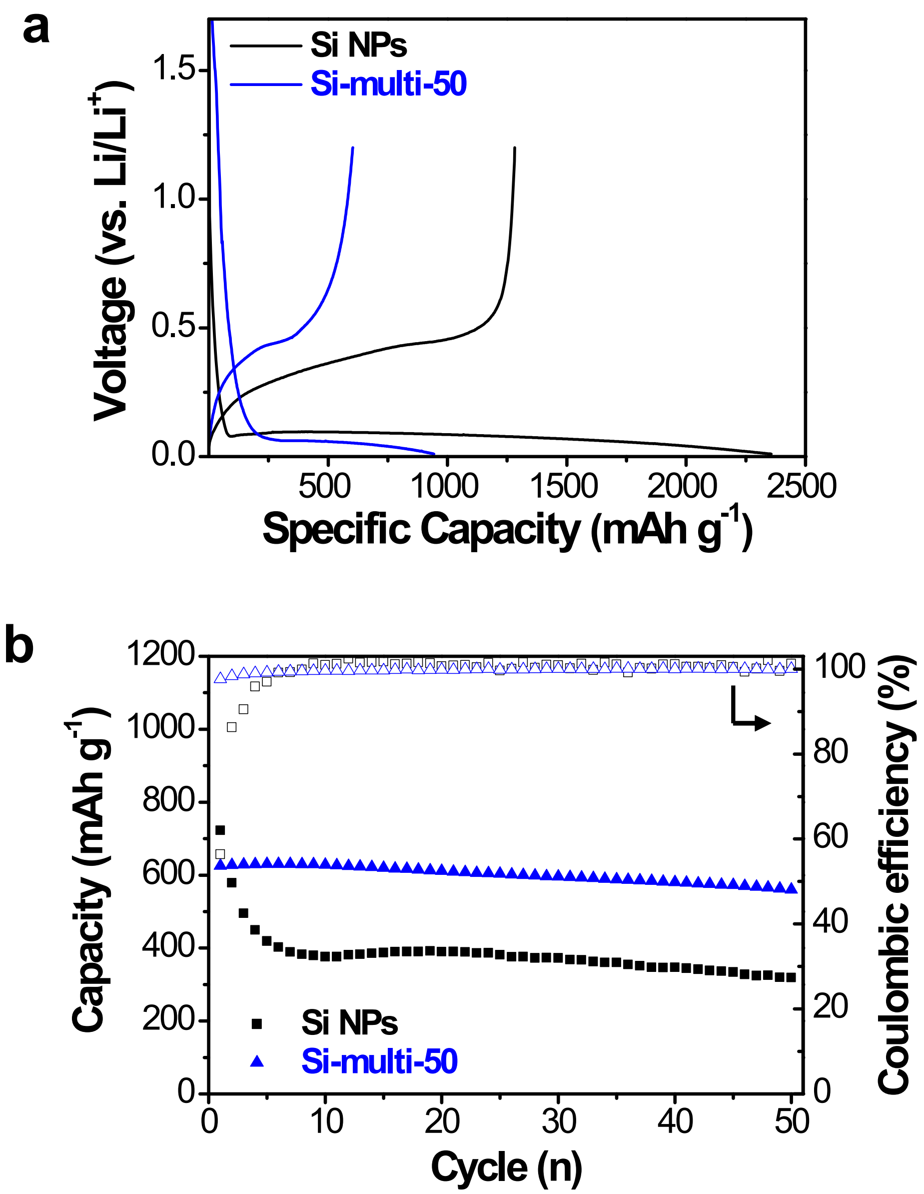

Figure S5. Electrochemical performances of pristine Si NPs and Si-multi-50 electrodes with high mass loading of 3 mg cm^{-2}. (a) First cycle voltage profiles of pristine Si and Si-multi-50 at rate of 0.05 C. (b) Cycling retentions of the pristine Si and the Si-multi-50 electrodes at rate of 0.1 C for 50 cycles. The Si-multi-50 thick electrode showed highly stable cycling retention, compared to the pristine Si NPs.

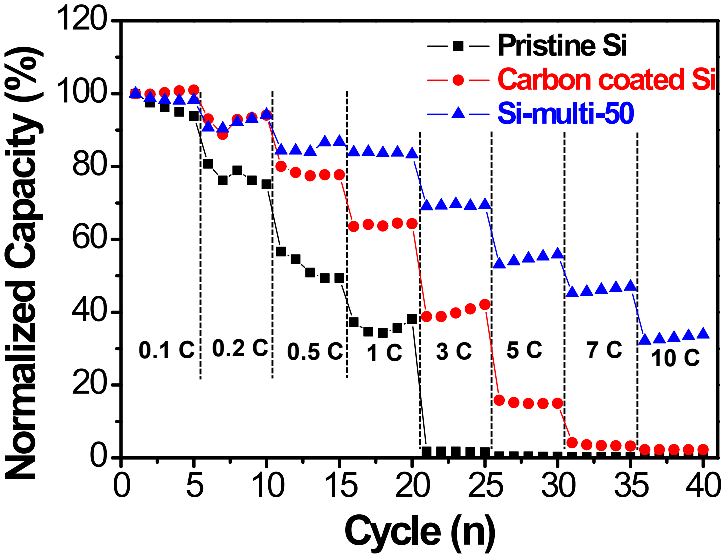

Figure S6. Rate capabilities of the pristine Si, carbon-coated Si, and Si-multi-50 electrodes obtained at various discharge rates with a fixed charge rate of 0.2 C. To clearly see the difference in the rate capability of the three different electrodes, the normalized capacity was used.

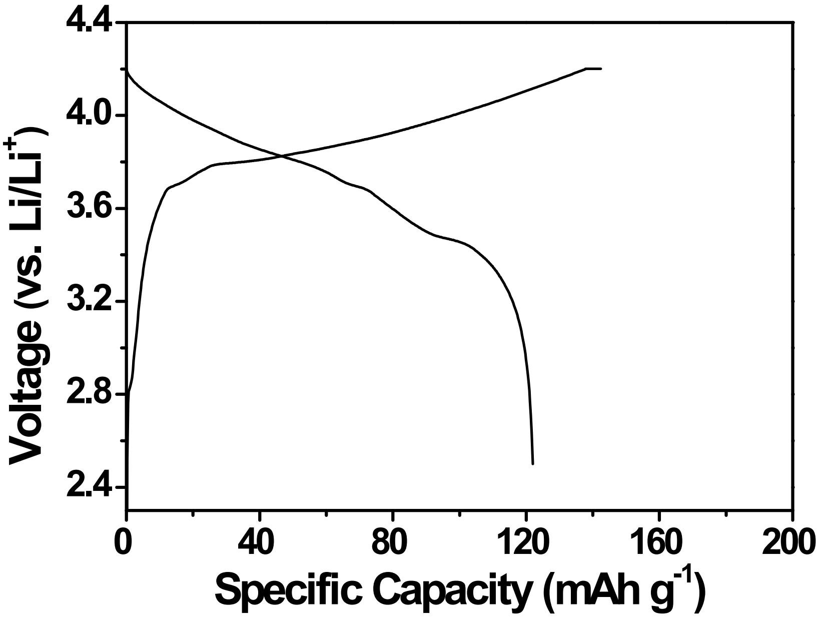

Figure S7. Voltage profile of Si-multi-50/$LiCoO_2$ electrode obtained at a rate of 0.1 C in the range of 2.5-4.2 V.

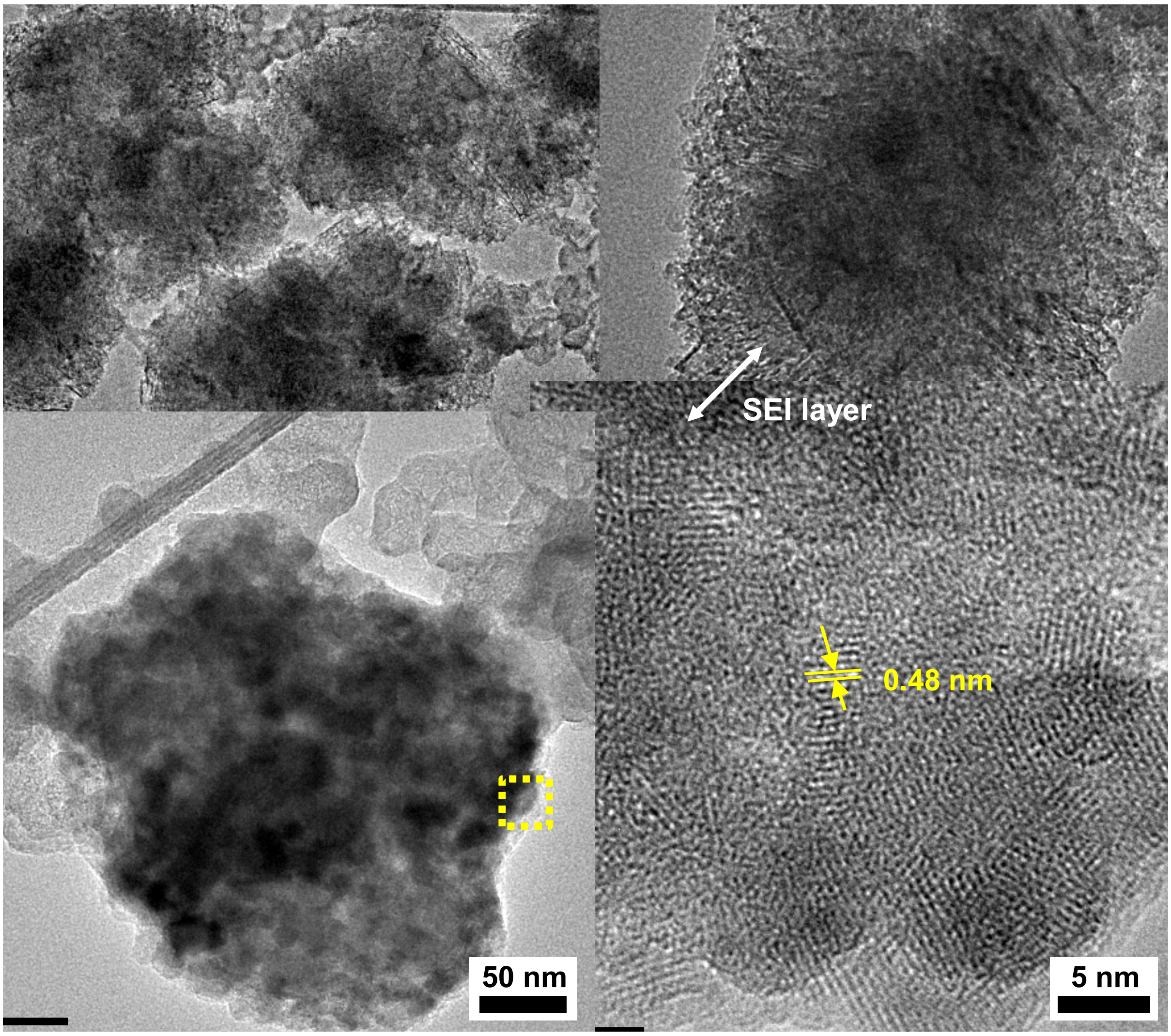

Figure S8. TEM images of (a, b) pristine Si particles and (c, d) Si-multi-50 particles after 100 cycles at 0.1 C. The pristine Si particles are seriously aggregated with thick SEI layers due to a large volume change during the repeated cycling, while the Si-multi-50 particles show slightly expanded structure with a thin SEI layer. In particular, lithium titanate layers are clearly seen even after 100 cycles (Fig. S6d), demonstrating that the lithium titanate acts as buffer layer for a large volume change of Si electrode.

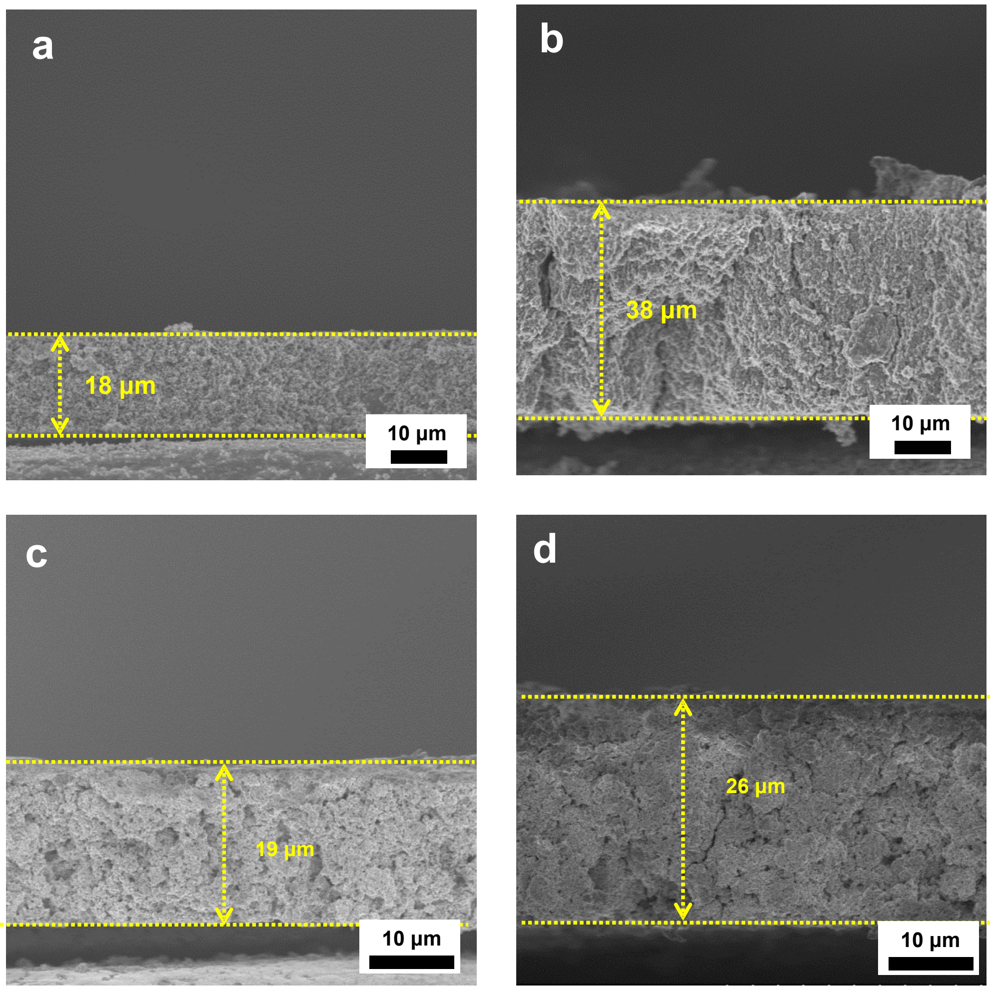

Figure S9. Cross-sectional SEM image of pristine Si electrode (a) before cycle and (b) after 100 cycles at 0.1 C rate. Cross-sectional SEM image of Si-mutli-50 (c) before cycle and (d) after 100 cycles at 0.1 C rate. The pristine Si electrode was expanded to 100 % after cycling, while the Si-multi-50 showed less volume expansion (37%). These results demonstrate that the multi-functional coating layers play a key role in reducing the volume expansion of Si by combining their good mechanical properties and formation of stable SEI layers on the Si surface.